1993

Using Electrochemical Impedance Spectroscopy as a Tool for Organic Coating Solute Saturation Monitoring

Branko N. Popov
University of South Carolina - Columbia, popov@engr.sc.edu

Mohammed A. Alwohaibi

Ralph E. White
University of South Carolina - Columbia, white@cec.sc.edu

Publication Info

Journal of the Electrochemical Society, 1993, pages 947-951.

Using Electrochemical Impedance Spectroscopy as a Tool for Organic Coating Solute Saturation Monitoring

B. N. Popov,* Mohammed A. Alwohaibi,[a] and R. E. White*

Department of Chemical Engineering, University of South Carolina, Columbia, South Carolina 29208

ABSTRACT

Electrochemical impedance spectroscopy (EIS) has been used to study the solute uptake for epoxy/phenolic (E/p) and epoxy/amine (E/a) thick-coated mild steel samples immersed for 160 days in 3.5 weight percent NaCl solution exposed to air. Samples with thicknesses of approximately 200 μm with an exposed surface area of 22.6 cm^2 were used to follow solute saturation of the organic coating. Good agreement was obtained between the calculated and measured coating capacitance when, according to the diffusion equation, the coating capacitance was plotted against exposure time.

Electrochemical impedance spectroscopy (EIS) has been used successfully to follow the degradation and to predict the life of organic coatings used to protect industrial structures.[1-5] Coatings at initial exposure time behave as dielectric material and show pure capacitor behavior.[1] It has been found that coating resistance decreases with time due to the gradual penetration of conductive electrolyte through the coating structure.[6-11] In addition, coating capacitance was found to be influenced by the amount of water uptake.[6-11] The coating capacitance *vs.* time curves in the early stages of exposure, prior to corrosion, have been utilized by many investigators to estimate the amount of water uptake in the coating.[13-17] In typical impedance investigations, the corrosion behavior of coatings with 20-50 μm thicknesses was studied.[6-11, 24-26] The objective of this investigation was to estimate the barrier properties of E/p and E/a thick deposits of approximately 200 μm in 3.5 weight percent (w/o) NaCl solution, which has been exposed to air for about 160 days.

Experimental

In order to measure coating characteristics using EIS, a special electrochemical cell made of a clear nonconductive plastic material shown in Fig. 1 was made. The exposed working electrode area was 22.6 cm^2 of mild steel coated with E/p and E/a coatings. The coated mild steel samples were obtained from the Dow Chemical Company. The experiments were run under free corrosion conditions in a stagnate 3.5% NaCl solution open to air. A platinum gauze served as the counterelectrode and a scanning electron microscopy (SCE) served as the reference electrode. EIS data were obtained using a PAR Model 273 potentiostat/galvanostat and a PAR Model 5301 A (a two-phase lock-in amplifier) interconnected by a National Instrument IEEE-488 General Purpose Interface Bus (GPIB) to an IBM PS/2. Data were stored and analyzed using PAR M378 software on an IBM PS/2. The frequency range of 1 mHz to 100 kHz was applied with an ac voltage signal varying by ±10 mV.

Results and Discussion

Figures 2 and 3 show representative Bode and phase shift plots, respectively, for coatings with thicknesses on the order of 200 μm exposed to the test solution for about 160 days. The data were fitted using two circuit-analog models shown in Fig. 4. The circuit analog model in Fig. 4a was used to fit the data obtained before saturation (it will be shown later that the saturation time takes between 25 and 30 days) of the epoxy coating with the solution. In Fig. 4b the phenomena occurring at the substrate/coating interface were taken into account and were used to analyze the data after the coatings were saturated with the electrolyte. The EIS data were fitted using Macdonald's complex nonlinear least squares algorithm, CNLS.[18]

Values of the initial coating capacitance C_o are shown in Table I for several coatings. Using the initial coating capacitance values and the thickness of the coatings, the dielectric constant for each coating was calculated by using the following equation

$$\epsilon = \frac{d}{\epsilon^o A} C_o \qquad [1]$$

where d is the coating thickness in cm, ϵ is the dielectric constant of the coating, A is the area of the test sample exposed to the electrolytic solution in cm^2, ϵ^o is the free space dielectric constant with a value of 8.85×10^{-14} F/cm, and C_o is the initial coating capacitance in F measured after 1 h of exposure. The average value of the initial dielectric constant is equal to 4, as shown in Table II. This value is typical for a dry coating,[6-11,24-26] indicating that initially a relatively low amount of electrolyte is adsorbed.

Fitted values of the coating pore resistance R_{po} as a function of exposure time in 3.5 w/o NaCl solution are shown in Fig. 5. The pore resistance of the samples has initially a high value in the order of 10^{10} Ω, which gradually decreases as the solution penetrates through and saturates the organic coating, indicating an increasing ionic conductivity of the coating. If the external portion of the epoxy coating has defects in the form of fissures and capillaries, one can expect a rapid decrease of pore resistance during the first few days corresponding to entry of solution into the capillaries. This phenomena was not observed in Fig. 5. Instead,

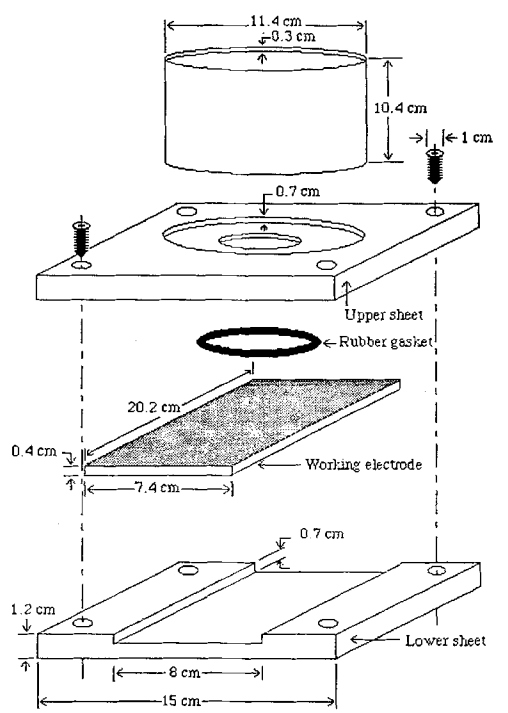

Fig. 1. Schematic of the test cell.

* Electrochemical Society Active Member.
[a] Present address: Al-Khobar 31952, Saudi Arabia.

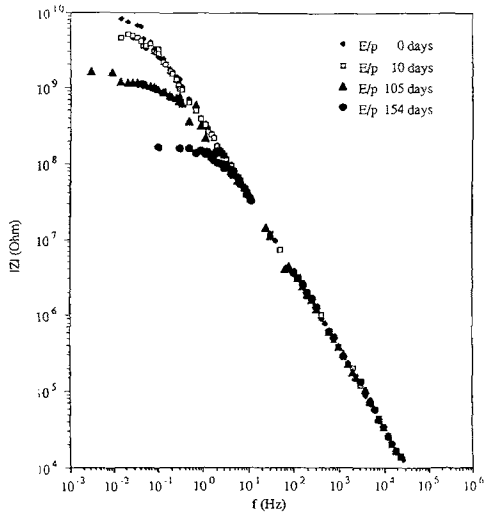

Fig. 2. Bode-magnitude plot for 0.0195 cm thick epoxy/phenolic-coated steel in 3.5 w/o NaCl solution for a period of five months.

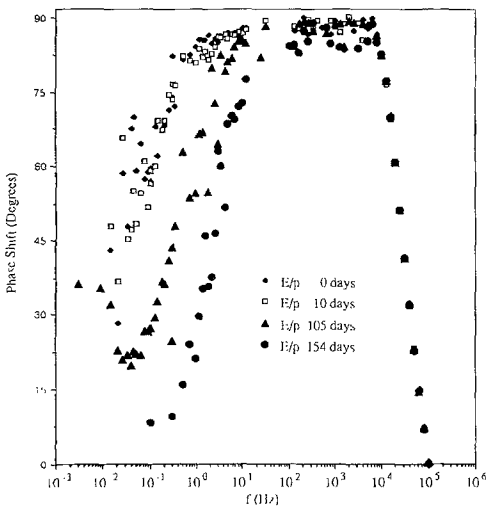

Fig. 3. Bode-phase plot for 0.0195 cm thick epoxy-coated steel in 3.5 w/o NaCl solution over period of five months.

for all coatings almost a linear decrease occurs which can be attributed to diffusion of solution into the epoxy coating. After about 30 days of exposure, the E/p and E/a samples with a thickness of 0.0195 cm and 0.0201 cm, respectively, show a sudden drop of the pore resistance indicating that the saturation of the coating with the electrolyte has occurred. The time required for diffusion of the electrolyte through the coating to the coated metal interface is proportional to the square of the thickness of the coating.[5] Consequently, as observed in Fig. 5, the E/p with a thickness of 0.0223 cm has greater pore resistance values, and the observed changes in pore resistance are less explicit than those observed for the other two coatings which have

Table I. Values of dielectric constants of coatings calculated from coating capacitance at initial exposure in 3.5 w/o NaCl solution.

Sample (type)	Thickness (μm)	C_o (F)	ϵ
1. E/p[a]	194.8	4.098×10^{-10}	4.054
2. E/a[b]	201.4	4.130×10^{-10}	4.222
3. E/p	223.0	3.422×10^{-10}	3.871

[a] Epoxy/phenolic
[b] Epoxy/amine.

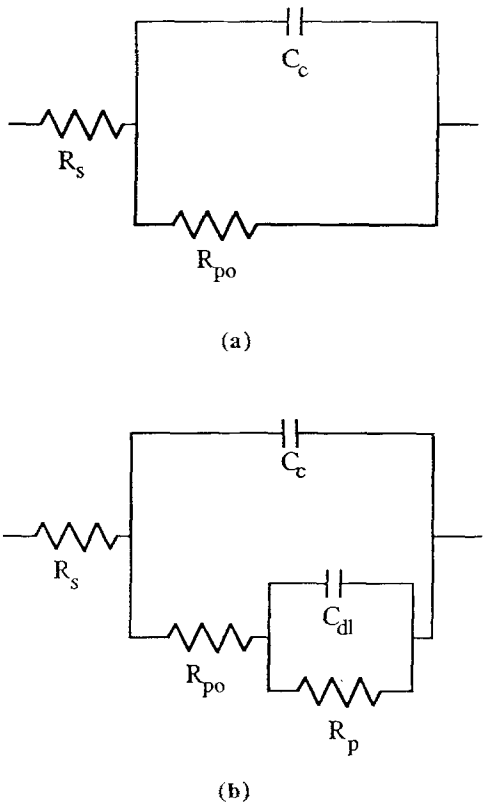

Fig. 4. Circuit analog modules used to fit EIS data, (a) circuit used to fit EIS data at initial exposure and (b) circuit used to fit EIS data after coating saturation.

smaller thicknesses. Also, as seen in Fig. 5, the E/p coating with a thickness of 0.0223 cm has a greater saturation time plateau indicating better stability and protective properties. The results in Fig. 5 also indicate that R_{po} decreases over time at different rates depending on the chemical composition of the coating. The R_{po} of the E/a coating decreases faster as a function of time when compared with the observed R_{po} decrease of E/p coating, indicating that E/p has better protective properties.

Figures 6-8 show the dependence of the coating capacitance on time for intact samples with various coating thicknesses. The coating capacitance increases monotonically indicating that the water uptake is diffusion controlled. In general, the coating capacitance increases for a value of 4.0×10^{-10} F. Mass uptake was calculated using the following equation

$$M_f = \rho_s X_V \quad [2]$$

where ρ_s is the 3.5 w/o NaCl solution density of 1.2176 g/cm^3 at 25° [19] and X_V is the volume fraction available within the coating defined as follows[6-11]

$$X_V = \frac{\log (C_c/C_o)}{\log (80)} \quad [3]$$

where C_c is the coating capacitance as a function of time and C_o is the initial coating capacitance obtained from EIS

Table II. Coating capacitance at saturation time, dielectric constant and ratio of saturation coating capacitance to initial coating capacitance.

Sample type	Saturation time (Days)	C_∞ (F)	ϵ_s	C_∞/C_o
1. E/p	26	4.630×10^{-10}	4.578	1.130
2. E/a	25	4.560×10^{-10}	4.661	1.104
3. E/p	30	3.904×10^{-10}	4.419	1.140

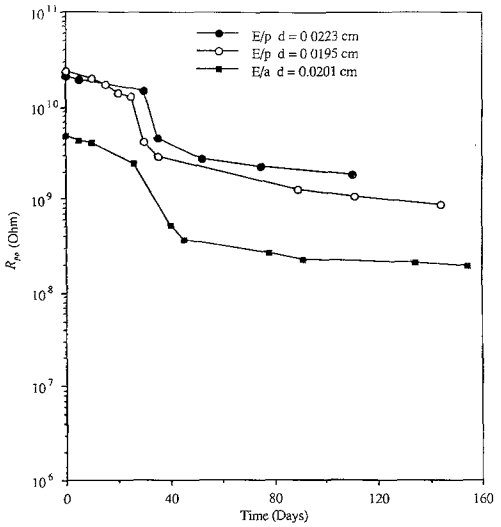

Fig. 5. Pore resistance of epoxy coated samples as a function of exposure time in 3.5 w/o NaCl solution.

data at initial exposure. In this analysis it is assumed that Na^+ and Cl^- diffuse at the same rate as water and oxygen. Using the coating capacitance values at saturation time (according to Fig. 6-8) and thickness of the coating, the dielectric constant when the coating is saturated with the solute was calculated and is presented in Table II. Equation 1 was used with the coating capacitance at saturation time to calculate the coating dielectric constant at saturation time ϵ_s. The ratio of coating capacitance measured at time t and the initially measured capacitance of the coating gives an indication of the extent of the adsorption. Thus, high ratio means that the coating adsorbs more solute. As seen in Table II only a small increase of the dielectric constant calculated at saturation time is observed, indicating that the coating is a good barrier with a small porosity. Accordingly, only a small fraction of the solute has been adsorbed.

In Fig. 9, the water uptake is correlated to the ratio of the experimentally measured coating capacitance and the initial (dry sample) coating capacitance according to Eq. 2. As is seen in Table II, the highest ratio C_∞/C_o of 1.140 has been observed for the sample with a thickness of 230.0 μm. A small increase of the coating capacitance after saturation time is observed. Initially, the measured coating capacitance ratio equals 1 with zero water uptake. When the actual measured values of C_∞/C_o were plotted (as in the enlarged portion in Fig. 9] as a function of water uptake, a linear dependence is observed, as expected according to Eq. 2. This is due to the small increase of the measured capacitance as exposure time increases. This behavior is expected, since only a small fraction of the curve in Fig. 9 is presented in the enlarged portion. Accordingly, small changes in coating capacitance are linearly related to the water uptake and hence to the concentration of the electrolyte in the pores of the coating. This has been experimentally shown to be valid for the epoxy/polyamide coatings.[20] This behavior suggests that the coating capacitance may be treated as a variable whose values may be determined by the diffusion equation[20-22]

$$\frac{\partial C_c}{\partial t} = D_{eff}\frac{\partial^2 C_c}{\partial x^2} \qquad [4]$$

The initial and boundary conditions are at

$$t = 0 \quad x \geq 0 : C_c = C_o \qquad [5]$$

For

$$t \geq 0 \quad x = 0 : C_c = C_\infty \qquad [6]$$

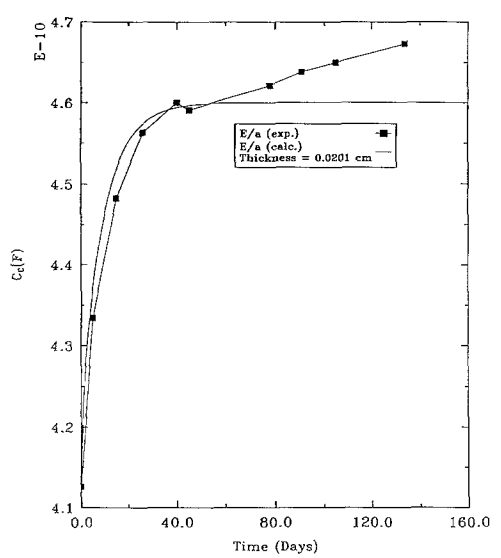

Fig. 6. Experimental and calculated coating capacitance as a function of exposure time in 3.5 w/o NaCl solution for epoxy/phenolic-coated steel.

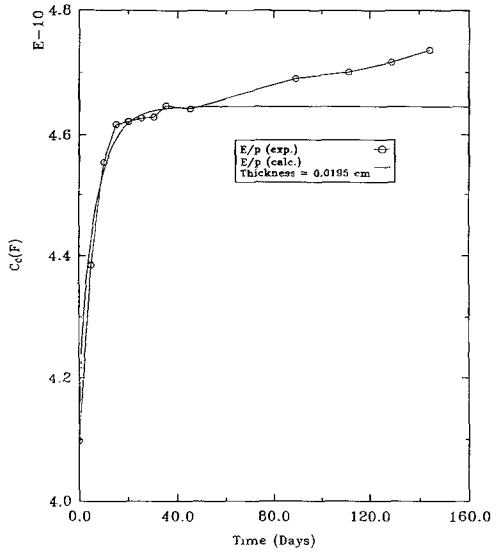

Fig. 7. Experimental and calculated coating capacitance as a function of exposure time in 3.5 w/o NaCl solution for epoxy/amine-coated steel.

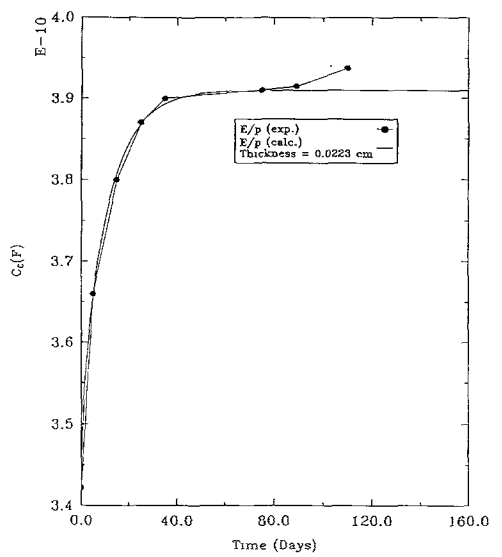

Fig. 8. Experimental and calculated coating capacitance as a function of exposure time in 3.5 w/o NaCl solution for epoxy/phenolic-coated steel.

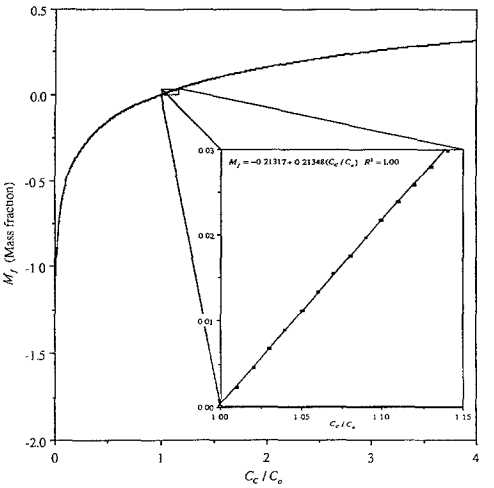

Fig. 9. Mass fraction *vs.* ratio of coating capacitance to initial coating capacitance.

and for

$$t \geq 0 \quad x = d : C_c = C_\infty \qquad [7]$$

To use Eq. 4 it is assumed that: (*i*) the solute volume fraction is evenly distributed along the diffusion path and that no empty spaces are available within the structure of the organic coating. (*ii*) Solute diffusion is one-dimensional and one directional. (*iii*) The diffusion coefficient is constant and is not a function of the amount of water adsorbed. (*iv*) The coating does not swell during the experiment and accordingly the coating thickness is constant. The analytical solution of Eq. 4 with the initial conditions given in Eq. 5, 6 and 7 is as follows[20]

$$\frac{C_c - C_o}{C_\infty - C_o} = 1 - 8/\pi^2 \sum_{n=0}^{\infty} \frac{\exp\{-D_{eff}(2n+1)^2(\pi/d)^2 t\}}{(2n+1)^2} \qquad [8]$$

The first four terms of the analytical solution (Eq. 8) were used to estimate the effective diffusion coefficient by using a SAS program (NLIN).[23] A nonlinear least squares fit of the normalized coating capacitance (*i.e.*, left side of Eq. 8) was used for all capacitance values until the saturation time for the coating was reached (around 30 days for most of the samples). Equation 8 was then utilized to generate the theoretical coating capacitance values of the coating, by using the same coating thickness as the thickness of the samples in Fig. 6-8. The theoretical coating capacitance values as a function of time are shown in Fig. 6-8, and the results are compared with the obtained experimental results. The theoretical coating capacitance increases with time in an expected exponential fashion. The observed increase of the coating capacitance is due to the water uptake by the coating. As shown in Fig. 6-8, the rate of change of the coating capacitance is high at the beginning but then slows as saturation occurs. Note that the measured coating capacitance is a combination of the organic coating capacitance and the adsorbed water capacitance. Taking into account that the dielectric constant of water is about 20 times that of the coating, one would expect a significant change of the coating capacitance during adsorption. The saturation time varies from 25 days for a sample with thickness of 201.4 μm up to 30 days for a sample with thickness of 223 μm as shown in Fig. 5. An interesting phenomena is observed in Fig. 6-8. The experimentally determined coating capacitance values continued to increase slowly even after saturation has occurred. This phenomena may be due to different water uptake rates or is due to the disbondment of the organic coating which depends on: (*i*) the rate of oxygen reduction and OH^- generation at the coating/metal interface and (*ii*) physicochemical processes which occur at the interface in the presence of the electrolyte. In the presence of the electrolyte at the interface, the reactions that occur are the oxidation of iron and reduction of oxygen and accordingly, one can expect the main contribution to coating disbondment to be due to OH^- generation. The coating capacitance measured at saturation time was used to calculate the solubility, *S*, of the electrolyte in the organic coating using Eq. 3.[6-11] A penetration coefficient was calculated using the equation

$$P = D_{eff} S \rho_s \qquad [9]$$

where ρ_s is the density of the 3.5 w/o NaCl solution at room temperature, *S* is the solubility coefficient of the chloride solution in the organic coating, and *P* is the penetration coefficient of the chloride solution.

Table III. Estimated effective diffusion, solubility, and penetration coefficients.

Sample (type)	Data from Figure	D_{eff} (cm^2/s)	*S* (%)	*P* (g/cm/s)
1. E/p	6	4.92×10^{-11}	2.260	1.14×10^{-12}
2. E/a	7	6.31×10^{-11}	2.770	1.79×10^{-12}
3. E/p	8	5.57×10^{-11}	3.007	1.68×10^{-12}

Table IV. Transport properties in organic coatings.

Species of interest	Diffusion coefficient (cm^2/s)	Ref.
O_2	10^{-10} to 10^{-8}	Brandrup and Immergut (Ref. 27)
Cl^-	0.47×10^{-11}	Glass and Smith (Ref. 28)
Na^+	0.31×10^{-10}	Glass and Smith (Ref. 28)

The estimated diffusion coefficient, the solubility coefficient as well as the penetration coefficient are presented in Table III. As one can see from Table III, almost the same diffusion coefficients were obtained for both E/p and E/a coatings. The transport properties data in epoxy polyamide coatings compiled from various references are given in Table IV. Water diffusivity depends upon the coating chemical composition and thickness and varies between 10^{-8} to 10^{-10} cm^2/s.[29] Denton *et al.*[20] have demonstrated for polyamide films that adsorbed moisture uptake is well approximated by a one-dimensional Fickian diffusion model, with a room temperature $D = 5 \times 10^{-9}$ cm^2/s. One can expect that migration may modify these times, since the electroactive species must accumulate to maintain electroneutrality. It has been pointed out by Leidheiser *et al.*[30] that the permeation rates for water and oxygen are in excess of that required to sustain cathodic reduction of oxygen at the coating/substrate interface and accordingly are not rate determining. The major ionic charge transport carrier in the coating is the sodium ion, which is rate controlling in the corrosion process.[30] According to Table III, similar values for solubility of the electrolyte in the coating and the solute penetration coefficient were obtained for the same thickness of E/p and E/a coatings.

Conclusions

A small increase in the dielectric constant at saturation time is observed, indicating that studied coatings are with a small porosity and are good barriers. As a consequence, the observed changes in coating capacitance are linearly related to the water uptake. The observations allow the coating capacitance to be a monitored variable in the diffusion equation. The theoretical coating capacitance values were obtained by assigning the same coating thickness as those of the tested samples. A good agreement has been obtained between the calculated and measured coating capacitance, when according to the diffusion equation, the coating capacitance was plotted against exposure time. However, after the saturation of the coating has been reached, the experimentally determined capacitance continues to increase slowly. The observed phenomena results from the disbondment of the coating as a consequence of the oxygen reduction and OH^- generation at the coating/

metal interface. Almost the same diffusion coefficients were observed for E/p and E/a coatings. The pore resistance of the samples has initially a high value of 10^{10} Ω and decreases linearly with time. This phenomena was attributed to diffusion to the solute into the epoxy coating.

Acknowledgments

The authors appreciate the financial support of this project by the Dow Chemical Company and the Offshore Technology Research Center. One of us (M. A. A.) received a student fellowship from the Saudi Arabian Cultural Mission to the U.S.A.

Manuscript submitted Aug. 24, 1992; revised manuscript received about Dec. 18, 1992.

The University of South Carolina assisted in meeting the publication costs of this article.

LIST OF SYMBOLS

A	total cell area, cm^2
C_C	coating capacitance, F
C_o	initial coating capacitance, F
C_∞	saturation coating capacitance, F
d	coating thickness, cm
D_{eff}	effective diffusion coefficient, cm^2/s
M_f	mass fraction, g/cm^3
P	penetration coefficient, g/cm/s
R_{po}	pore resistance, Ω
S	solubility coefficient, %
X_V	volume fraction

Greek

ϵ	coating dielectric constant
ϵ_s	saturated coating dielectric constant
ϵ^o	free space dielectric constant = 8.85×10^{-14}, F/cm
ϵ_{water}	dielectric constant of water
ρ_s	density of solution, g/cm^3

REFERENCES

1. M. W. Kendig, F. Mansfeld, and S. Tsai, *Corros. Sci.*, **23,** 317 (1983).
2. H. P. Hack and J. R. Scully, *This Journal,* **138,** 33 (1991).
3. S. Haruyama, M. Sari, and T. Tsuru, in *Corrosion Protection by Organic Coatings,* M. W. Kendig and H. Leidheiser, Jr., Editors, PV 87-2, p. 197, The Electrochemical Society Softbound Proceedings Series, Pennington, NJ (1986).
4. H. Leidheiser and W. Wang, in *Corrosion Control by Organic Coatigs,* H. Leidheiser, Jr., pp. 70-77, NACE, Houston, TX (1981).
5. J. R. Scully, *This Journal,* **136,** 4 (1989).
6. F. Mansfeld, M. W. Kendig, and S. Tsai, *Corrosion,* **38,** 478 (1982).
7. W. J. Lorenz and F. Mansfeld, *Corros. Sci.,* **21,** 647 (1984).
8. F. Mansfeld, *Corrosion,* **44,** 856 (1988).
9. H. Leidheiser, Jr., *ibid.,* **39,** 189 (1983).
10. W. S. Tait, *J. Coat. Technol.,* **46,** 768 (1989).
11. M. Kendig and H. Leidheiser, Jr., *This Journal,* **123,** 982 (1976).
12. H. Leidheiser, Jr., R. D. Granata, and S. Turosy, *Corrosion,* **43,** 296 (1987).
13. D. M. Brasher and J. T. Nurse, *J. Appl. Chem.,* **9,** 96 (1959).
14. D. M. Brasher and A. H. Kingsbury, *J. Appl. Chem.,* **4,** 62 (1954).
15. R. E. Touhsaent and H. Leidheiser, Jr., *Corrosion,* **28,** 435 (1972).
16. H. Leidheiser, Jr., and M. W. Kendig, *ibid.,* **32,** 69 (1976).
17. S. A. Lindquist, *Corrosion,* **39,** 69 (1985).
18. J. R. Macdonald, *J. Electroanal. Chem.,* **223,** 25 (1987).
19. R. H. Perry and C. H. Chilton, *Chemical Engineering Handbook,* 5th ed., McGraw-Hill, Inc., New York (1973).
20. D. D. Denton, D. R. Day, D. F. Priore, and S. D. Senturia, *J. Electron. Mater.,* **14,** 119 (1985).
21. C. A. Carpenter and A. O. Fisher, *Mater. Perform.,* **20,** 40 (1981).
22. E. M. Rosen and D. C. Silvermann, *Corrosion,* **46,** 945 (1990).
23. *SAS/Users's Guide,* 1979 ed., SAS Institute Inc., Cary, NC (1979).
24. F. Mansfeld, C. H. Tsai, and H. Shih, in *Advances in Corrosion Protection by Organic Coatings,* D. Scantlbury and M. Kendig, Editors, PV 89-13, p. 288, The Electrochemical Society Softbound Proceedings Series, Pennington, NJ (1989).
25. S. A. McCluney, S. N. Popova, B. N. Popov, R. E. White, and R. B. Griffin, *This Journal,* **139,** 1556 (1992).
26. S. N. Popova, B. N. Popov, R. E. White, and D. Drazic, *Corrosion,* **46,** 1007 (1990).
27. *Polymers Handbook,* 2nd Ed., J. Brandrup and E. H. Immergut, Editors, John Wiley & Sons, Inc., New York (1975).
28. A. L. Glass and J. Smith, *J. Paint. Technol.,* **39,** 490 (1969).
29. R. T. Ruggeri and T. R. Beck, *Corrosion,* **39,** 452 (1983).
30. H. Leidheiser, Jr., D. J. Mills, and W. Bilder, in *Corrosion Protection by Organic Coatings,* M. W. Kendig and H. Leidheiser, Jr., Editors, PV 87-2, p. 31, The Electrochemical Society Softbound Proceedings Series, Pennington, NJ (1987).

Mechanisms of Passivity of Nonequilibrium Al-W Alloys

G. D. Davis,*[a] B. A. Shaw,*[b] B. J. Rees,[a] and M. Ferry[b]

[a] *Martin Marietta Laboratories, Baltimore, Maryland 21227*
[b] *The Pennsylvania State University, University Park, Pennsylvania 16802*

ABSTRACT

Sputter-deposited Al-W alloys exhibit considerably enhanced resistance to pitting corrosion over a range of pHs extending from pH 0 to 9.6. Surface analysis showed that although very little oxidized W is found in the passive film at near-neutral pHs, at pH 3 there are comparable amounts of oxidized W and Al. A review of the different mechanisms proposed to explain the passivity of this class of alloys suggests that the pitting resistance of Al-W is likely to result from inhibition and repassivation of pits due to the stability of oxidized W in low-pH environments as described by the solute-rich interphase model (SRIM).

Aluminum and its conventional alloys are susceptible to localized attack in chloride containing environments. Although the corrosion resistance of steels can be dramatically improved by the incorporation of chromium, molybdenum, and other elements to make stainless steels, there are no equivalent conventional stainless aluminum alloys. The failure to produce such alloys is largely due to the very low solubility of passivating species in aluminum; above a small fraction of an atomic percent, these species form precipitates and the microgalvanic couples established between the two phases lead to enhanced corrosion.

In the last several years, supersaturated aluminum alloys with Mo, Cr, Ta, W, Zr, Nb, Zn, V, Cu, Ti, and Si have been produced by several groups using rapid solidification or

* Electrochemical Society Active Member.